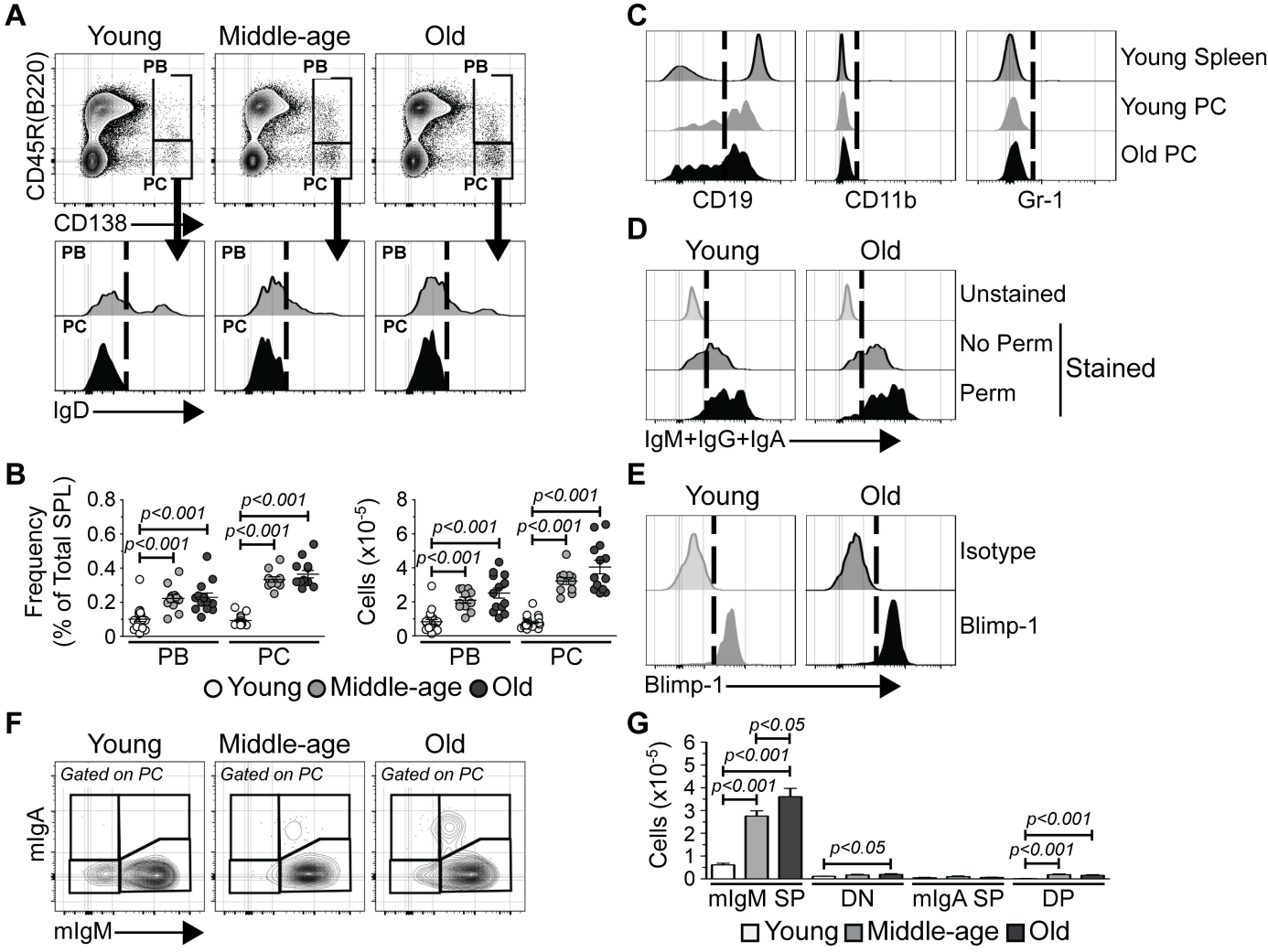

Figure S1 (Related to Figure 1). Plasmablasts and Plasma Cells Accumulate in the Aging Spleen
(A) Representative FACS plots depicting immunostaining of PBs and PCs in the spleens of young, middle-aged and old mice. Vertical dashed lines on IgD histograms depict cut-offs for positive staining. (B) Frequencies (left) and numbers (right) of PBs and PCs in the spleens of young, middle-aged and old mice. Each symbol represents an individual mouse. Animals used: Young = 21; Middle-aged = 11; Old = 13. (C) Representative FACS plots depicting CD19, CD11b and Gr-1 immunostaining of PCs in the spleens of young and old mice. Young total spleen is shown for comparison. Vertical dashed lines on histograms depict cut-offs for positive staining. (D) Representative FACS plots depicting IgM+IgA+IgG immunostaining of PCs in the spleens of young and old mice. Unstained samples are shown for comparison. Vertical dashed lines on histograms depict cut-offs for positive staining. No Perm = unpermeabilized samples, Perm = permeabilized samples. (E) Representative FACS plots depicting isotype control and Blimp-1 immunostaining of PCs in the spleens of young and old mice. Vertical dashed lines on histograms depict cut-offs for positive staining. (F) Representative FACS plots depicting mIgM and mIgA immunostaining of PCs in the spleens of young, middle-aged and old mice. (G) Numbers of SP, DN or DP mIgM$^+$ and/or mIgA$^+$ PCs in the spleens of young, middle-aged and old mice. Bars represent mean ± SEM. Animals used: Young = 21; Middle-aged = 11; Old = 13. (C-E) Data are representative of results from 2-4 animals. (B, G) SPL = spleen; Statistics: One-way ANOVA with Bonferroni's correction. Statistically significant p-values are indicated.
See also Figure 1.

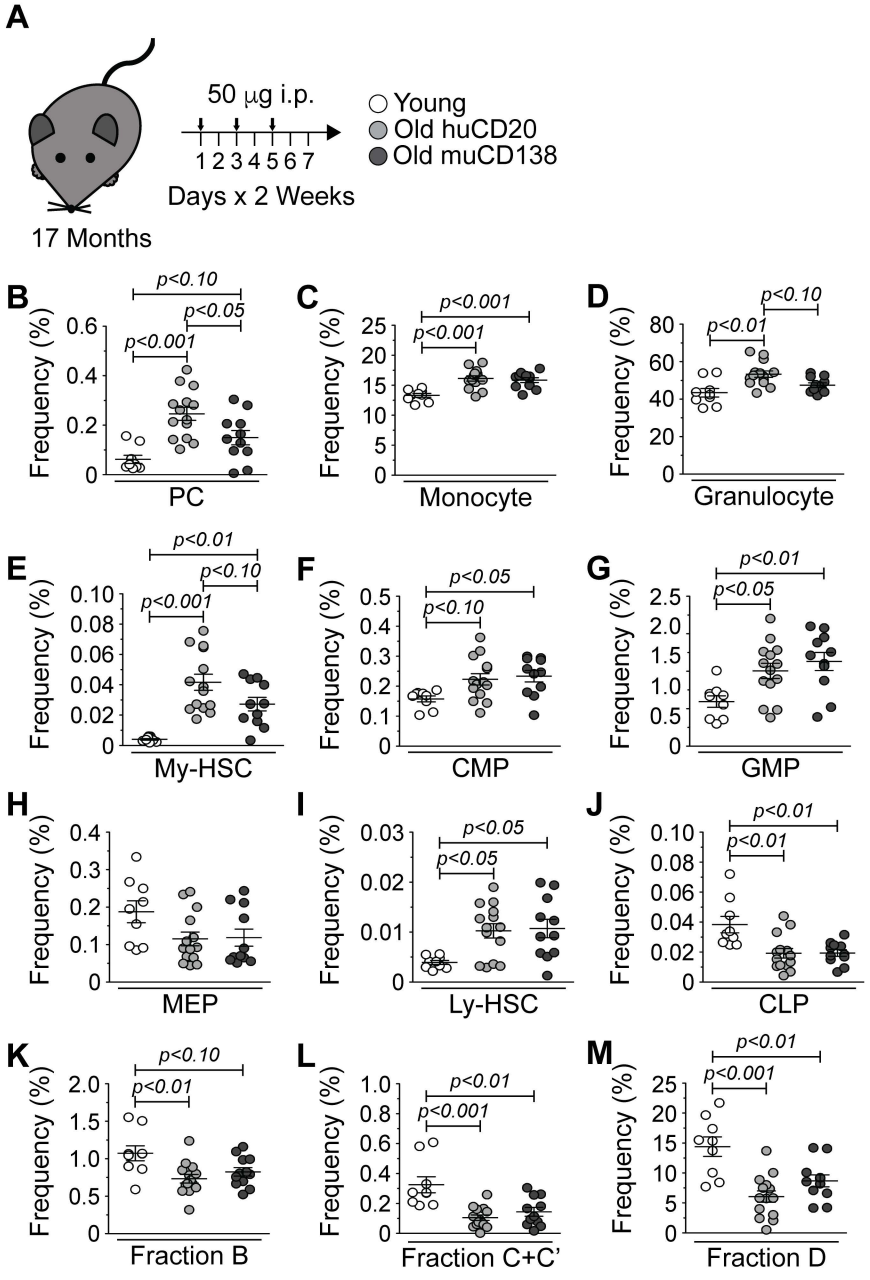

Figure S2 (Related to Figure 2). Frequencies of Hematopoietic Populations in the Bone Marrow of Young, huCD20 and muCD138 Treated Old Mice

(A) Schematic of antibody-mediated depletion of plasma cells in old mice. Old (17 months) mice received an intraperitoneal (i.p.) injection of 50 μg of either mouse anti-human CD20 (huCD20) or mouse anti-mouse CD138 (muCD138) antibodies three times per week for two weeks. Arrows indicate days of injection. (B) Frequencies of PCs in young and huCD20 and muCD138 treated old mice. (C, D) Frequencies of (C) monocytes and (D) granulocytes in young and huCD20 and muCD138 treated old mice. (E) Frequencies of My-HSCs in young and huCD20 and muCD138 treated old mice. (F-H) Frequencies of (F) CMPs, (G) GMPs and (H) MEPs in young and huCD20 and muCD138 treated old mice. (I) Frequencies of Ly-HSCs in young and huCD20 and muCD138 treated old mice. (J) Frequencies of CLPs in young and huCD20 and muCD138 treated old mice. (K-M) Frequencies of (K) Fraction B early pro-B, (L) Fraction C+C' late pro-B/large pre-B and (M) Fraction D small pre-B cells in young and huCD20 and muCD138 treated old mice. (B-M) Each symbol represents an individual mouse. Animals used: Young = 9; huCD20 = 14; muCD138 = 11. Statistics: One-way ANOVA with Bonferroni's correction. Statistically significant p-values are indicated.

See also Figure 2.

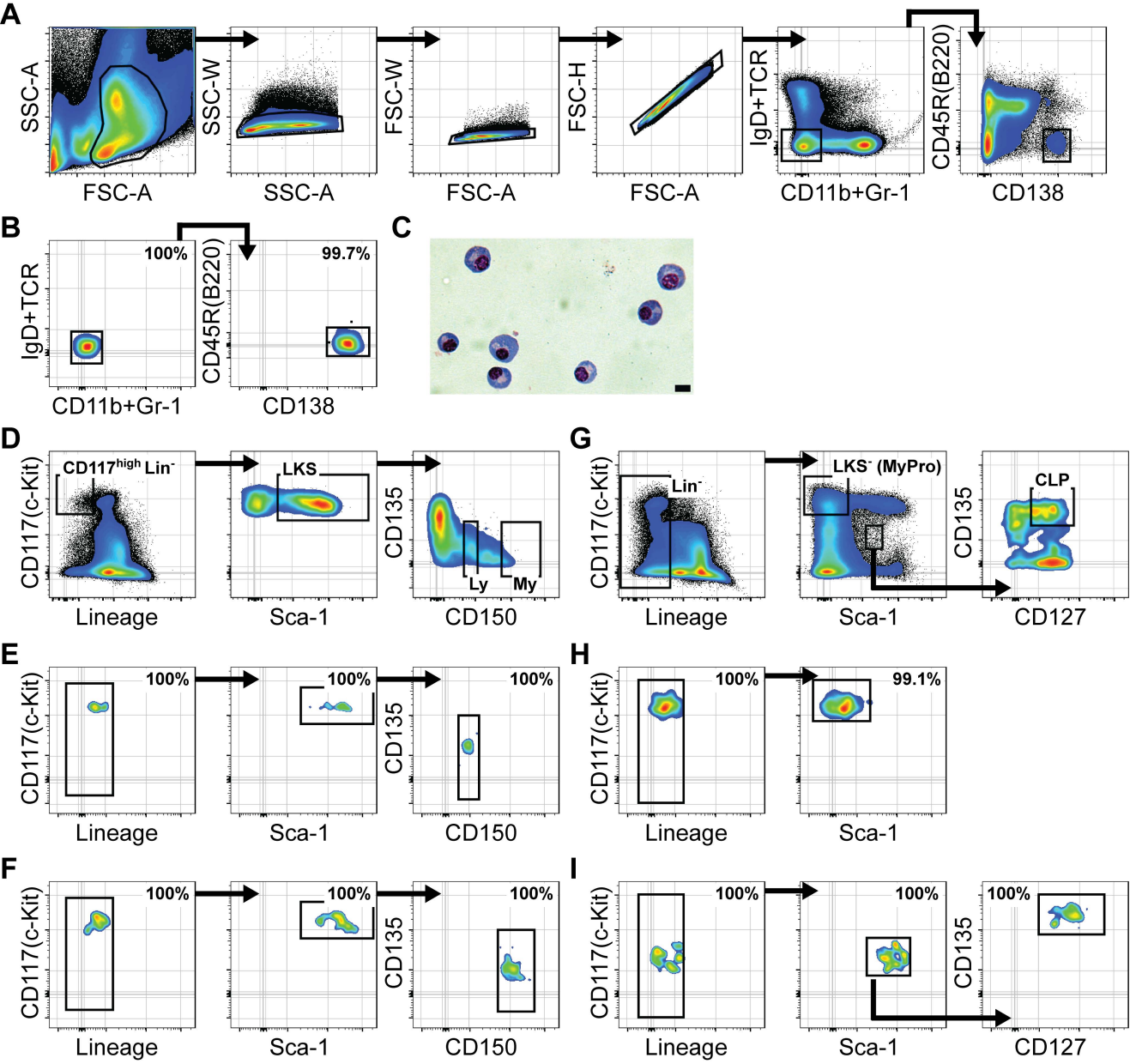

Figure S3 (Related to Figures 2, 4 and 5). FACS-sorting Strategies and Post-sort Purities for Plasma Cells, Hematopoietic Stem Cell Subsets, Myeloid Progenitors and Common Lymphoid Progenitors

(A) Sorting strategy for bone marrow PCs. TCR = TCRβ and TCRγδ. (B) Post-sort purity of PCs sorted in (A). (C) Photomicrograph of sorted PCs from (B). Cells were visualized with a 50x H_2O immersion objective and images captured using an Olympus DP12 camera. Scale bar represents 10 μm. (D) Sorting strategy for lymphoid-biased (Ly) and myeloid-biased (My) HSCs. Lineage (Lin) cocktail = CD48, CD3ε, CD8α, TCRβ, TCRγδ, NK1.1, Gr-1, TER-119, B220 and IgM. (E) Post-sort purity of Ly-HSCs sorted in (D). (F) Post-sort purity of My-HSCs sorted in (D). (G) Sorting strategy for MyPros and CLPs. Lin cocktail = CD3ε, CD8α, TCRβ, TCRγδ, NK1.1, Gr-1, TER-119, B220 and IgM. (H) Post-sort purity of MyPros sorted in (G). (I) Post-sort purity of CLPs sorted in (G).

See also Figures 2, 4 and 5.

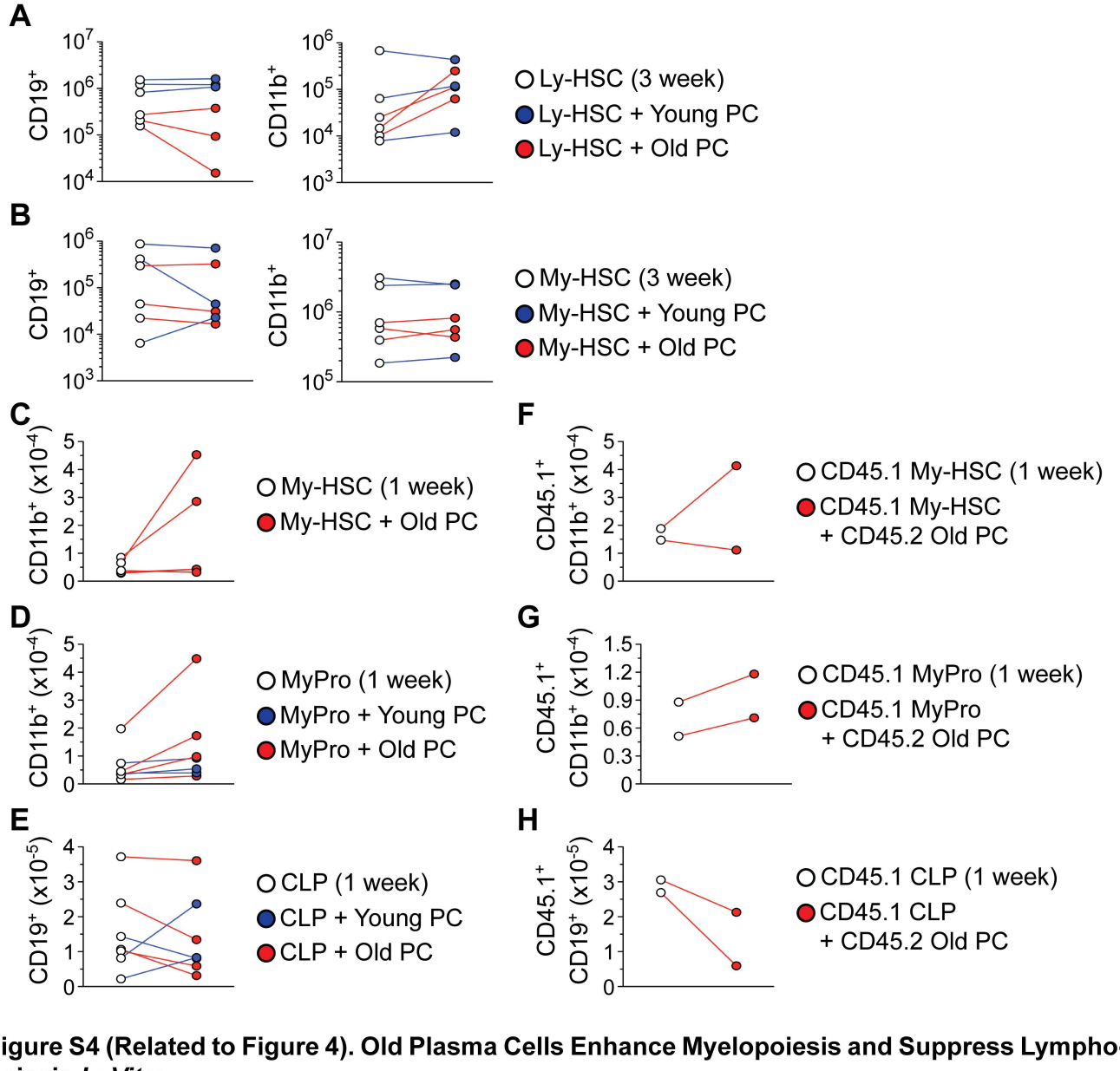

Figure S4 (Related to Figure 4). Old Plasma Cells Enhance Myelopoiesis and Suppress Lymphopoiesis *In Vitro*

(A) Numbers of $CD19^+$ (left) and $CD11b^+$ (right) cells produced in 3 week Ly-HSC cultures. (B) Numbers of $CD19^+$ (left) and $CD11b^+$ (right) cells produced in 3 week My-HSC cultures. (C) Numbers of $CD11b^+$ cells produced in 1 week My-HSC cultures. (D) Numbers of $CD11b^+$ cells produced in 1 week MyPro cultures. (E) Numbers of $CD19^+$ cells produced in 1 week CLP cultures. (F) Numbers of $CD45.1^+$ $CD11b^+$ cells produced in 1 week My-HSC cultures. (G) Numbers of $CD45.1^+$ $CD11b^+$ cells produced in 1 week MyPro cultures. (H) Numbers of $CD45.1^+$ $CD19^+$ cells produced in 1 week CLP cultures. (A-H) Lines indicate paired results from within individual experiments derived from 3-5 technical replicates per culture.

See also Figure 4.

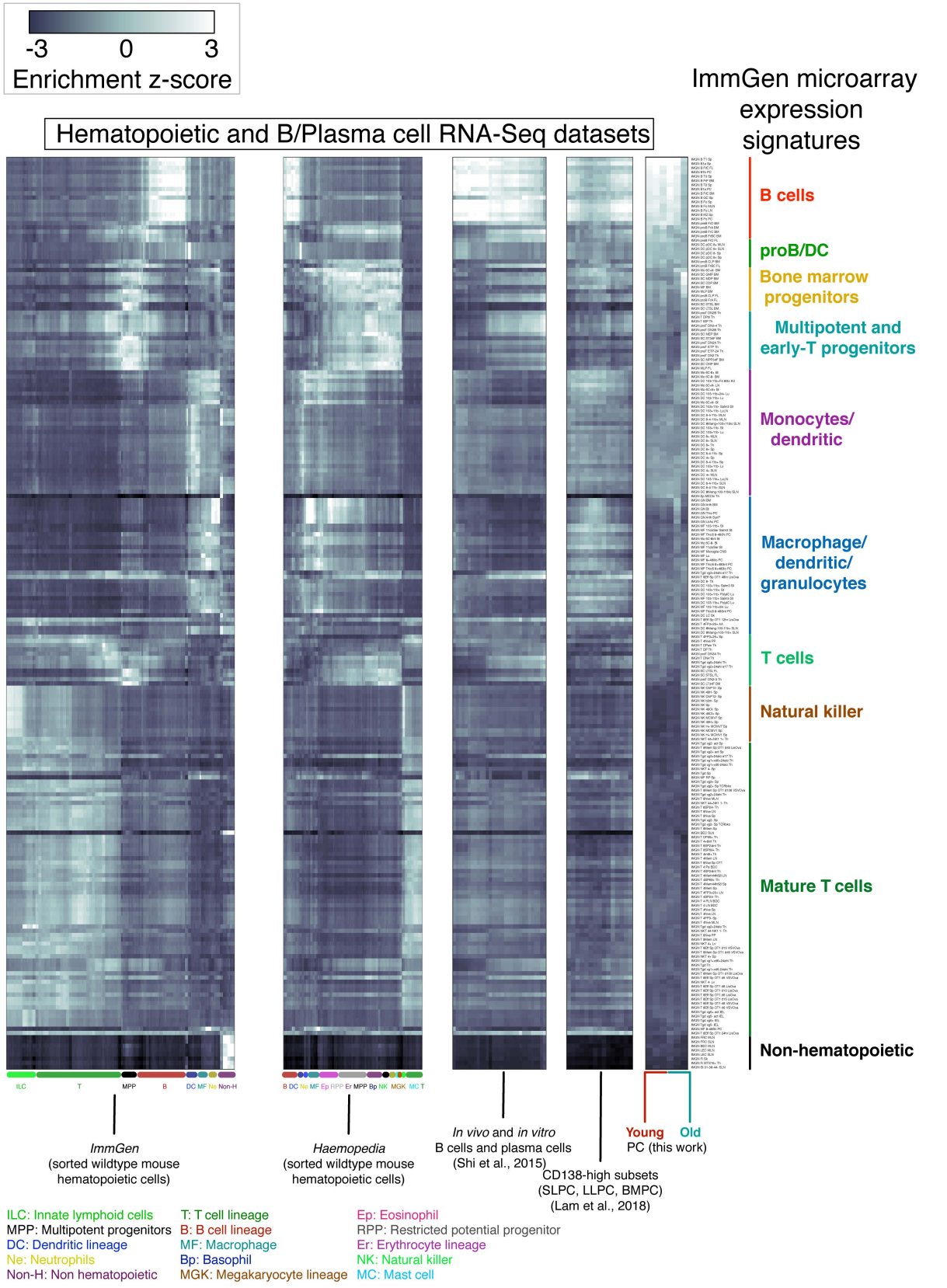

Figure S5 (Related to Figure 5). SaVanT enrichment scores for the plasma cell RNA-sequencing samples in this study using the expression signatures from the Immunological Genome Project

Shown are relative enrichment scores (normalized as z-score across all ImmGen signatures in the y-axis) for 5 independent gene expression datasets including the one presented in this work. The first two groups include data for a diverse panel of hematopoietic cell types that we use to address levels of specificity across different cell types. Two additional datasets comprise different subtypes of *in vitro* and *in vivo* B and plasma cells (Shi et al., 2015, Lam et al., 2018). ImmGen signatures in the y-axis are sorted top-to-bottom by the average relative enrichment score obtained for the samples presented in this work.

See also Figure 5.